OPTICAL TRANSFER FUNCTION

OF STARLETTE RETROREFLECTOR ARRAY

Technical Report

RTOP 161-05-02

Grant NGR 09-015-002

Supplement No. 57

Author: David A. Arnold

February 1975

Prepared for

National Aeronautics and Space Administration
Washington, D.C. 20546

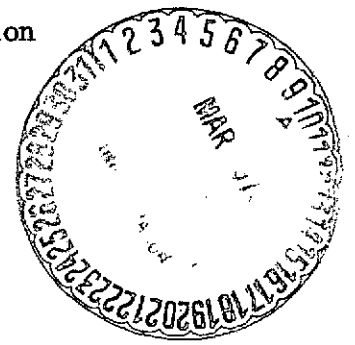

Smithsonian Institution
Astrophysical Observatory
Cambridge, Massachusetts 02138

The Smithsonian Astrophysical Observatory
and the Harvard College Observatory
are members of the
Center for Astrophysics

OPTICAL TRANSFER FUNCTION

OF STARLETTE RETROREFLECTOR ARRAY

Technical Report

RTOP 161-05-02

Grant NGR 09-015-002

Supplement No. 57

Author: David A. Arnold

February 1975

Prepared for

National Aeronautics and Space Administration
Washington, D. C. 20546

Smithsonian Institution
Astrophysical Observatory
Cambridge, Massachusetts 02138

The Smithsonian Astrophysical Observatory
and the Harvard College Observatory
are members of the
Center for Astrophysics

501-065

TABLE OF CONTENTS

ILLUSTRATIONS

TABLES

ABSTRACT

This report covers work done under NASA Grant NGR 09-015-002 Supplement No. 57. An optical transfer function has been computed for the retroreflector array carried by the Starlette satellite (1975 10A). The range correction is given for extrapolating laser range measurements to the center of mass of the satellite. The gain function and active reflecting area of the array have been computed for estimating laser-echo signal strengths.

OPTICAL TRANSFER FUNCTION OF STARLETTE RETROREFLECTOR ARRAY

Technical Report
RTOP 161-05-02

1. INTRODUCTION

This is the third in a series of reports giving optical transfer functions for satellites with retroreflector arrays. The first, performed under NASA Grant NGR 09-015-196, presented results calculated for the BE-B, BE-C, Geos 1, Geos 2, D1C, D1D, and Peole satellites. The second report gave results for the NTS-1 array (1974 056A); that work was supported by Grant NGR 09-015-002 Supplement No. 57. The development of computer programs used in these analyses was begun under Grant NGR 09-015-164, "Use of a Passive Stable Satellite for Earth Physics Applications."

Data on the Starlette satellite were obtained from the Centre National d'Etudes Spatiales, Toulouse, France.

2. ARRAY COORDINATE SYSTEM

The position and orientation of each cube corner in the array are given by the six numbers, x, y, z, θ, ϕ, α. The origin of the x-y-z coordinate system is the center of the satellite. The angles θ and ϕ are given in an x′-y′-z′ coordinate, which is parallel to the x-y-z system (Figure 1a). The angle α is shown in Figure 1b. The β and γ axes point east and north, respectively; in other words, γ is in the direction of decreasing ϕ, and β is in the direction of increasing θ.

501-065

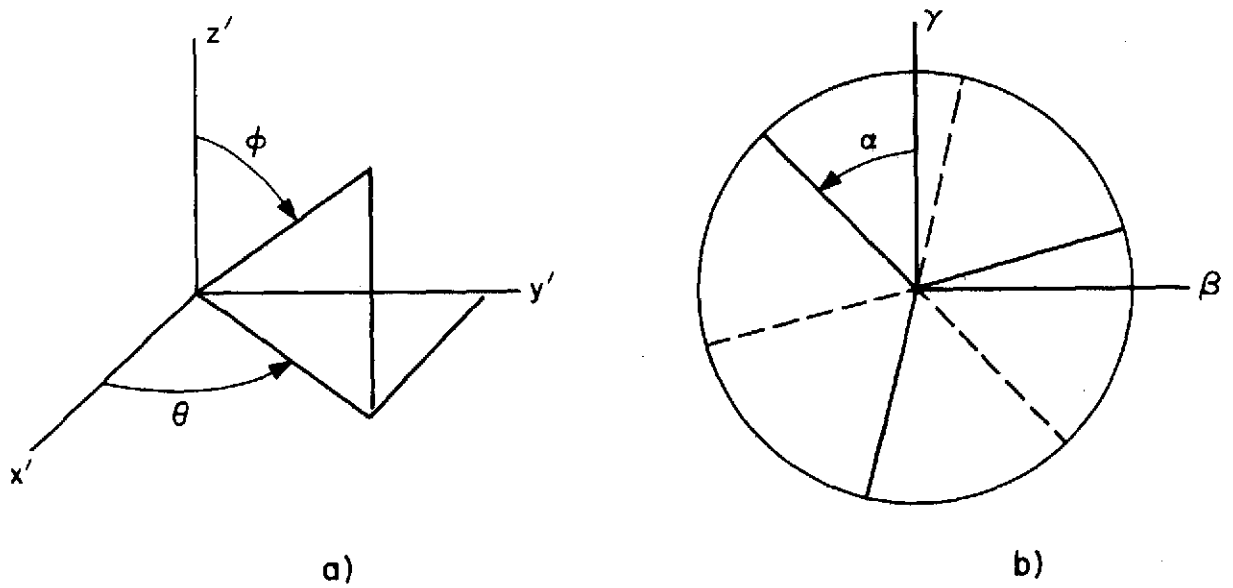

Figure 1. Coordinate system for cube-corner orientation.

3. RETROREFLECTOR SPECIFICATIONS

The cube corners used on Starlette have a circular face 32.8 mm in diameter, with a 23.3-mm length from the vertex to the face. The material is fused silica, and the reflecting faces are silver coated. The dihedral angles between the back faces are offset from 90° to provide the necessary beam divergence to account for velocity aberration. The specifications on the angular offset of the reflected beam from the cube corners are as follows:

Average offset = 7 arcsec,

50% between 5 and 9 arcsec,

100% between 0 and 10 arcsec.

The beam divergence is related to the dihedral-angle offset by the formula

$$\theta = 4\sqrt{2/3}\, n\delta \quad ,$$

where

θ = angular offset of reflected beam,

n = index of refraction of fused silica (1.457),

δ = offset of dihedral angles from 90°.

The dihedral-angle offsets corresponding to the offsets of the reflected beam listed in the specifications have been calculated and are listed in Table 1.

Table 1. Cube-corner specification conversion.

Offset of reflected beam (arcsec)	Dihedral-angle offset (arcsec)
0°	0.00
5	1.05
7	1.47
9	1.89
10	2.10

4. GEOMETRY OF THE ARRAY

The Starlette retroreflector array consists of 60 cube corners mounted on a 24-cm ball. The core of the satellite is an icosahedron. Each of the 20 triangular faces of the core is covered by a spherical cap containing three cube corners (see Figure 2). A detailed geometrical analysis of the core is given in the document "Project STARLET - Etude Geometrique de la Structure Porteuse de Reflecteurs Laser," Centre Nationale D'Etudes Spatiales Publ. No. 645, Toulouse, France, 27 October 1972.

501-065

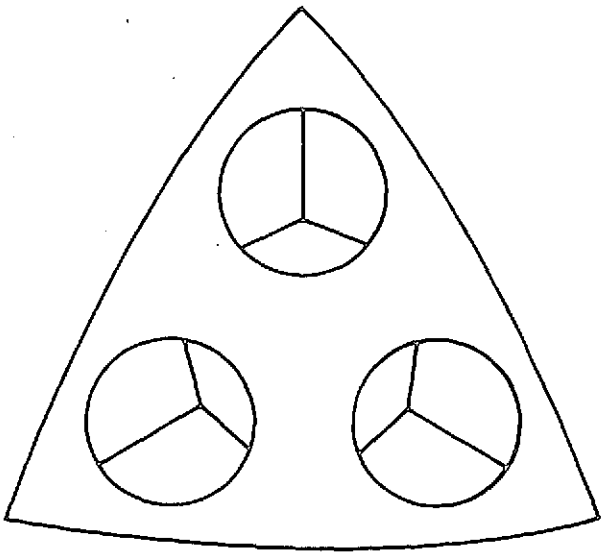

Figure 2. Orientation of reflectors on each face.

The cube corners are recessed below the surface by 0.5 ± 0.2 mm. The recess, together with the fact that the surface of the cube corner is flat, places the center of the front face of the cube corner closer to the center of the satellite than the 12-cm radius of the satellite. In the diagram below,

R = satellite radius (120 mm),

r = cube-corner radius,

= 32.8/2 = 16.4 mm,

D = distance from center of satellite to center of front face of cube corner

$$= \sqrt{(R - 0.5)^2 - r^2} = \sqrt{119.5^2 - 16.4^2} = 118.37 \text{ mm.}$$

501-065

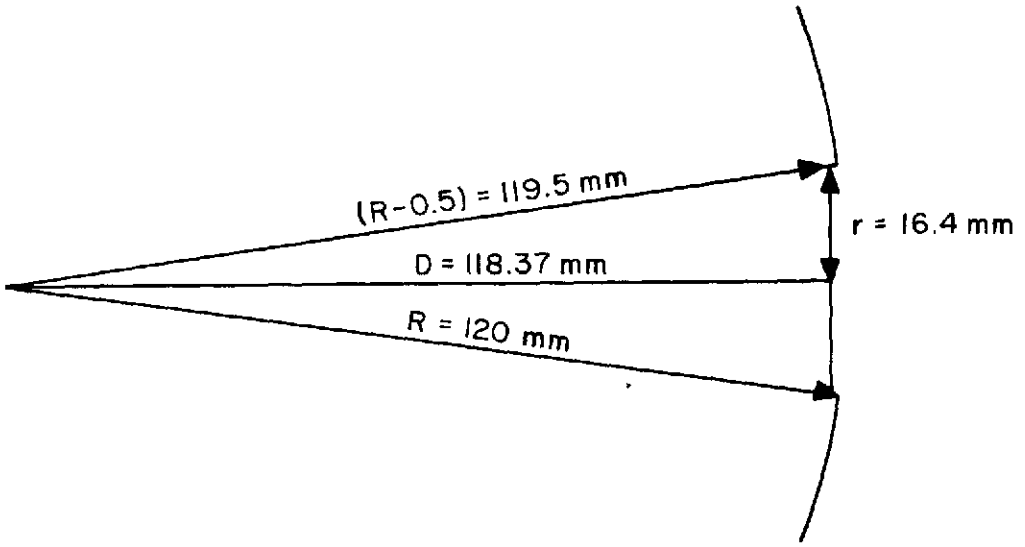

Table 2 lists the coordinates, in meters, of the center of the front face and the orientation angles, in degrees, for each cube corner. The first column gives the index identifying each of the 20 faces, and the second indexes the three retroreflectors on each face.

Table 2. Cube-corner positions and orientations.

CAP	RETRO	X	Y	Z	THETA	PHI	ALPHA
1	1	.04509	-0.00000	.10944	0.000	22.393	0.000
1	2	.08157	-.02651	.08157	342.000	46.437	133.487
1	3	.08157	.02651	.08157	18.000	46.437	226.513
2	1	.01393	.04289	.10944	72.000	22.393	0.000
2	2	.05042	.06939	.08157	54.000	46.437	133.487
2	3	0.00000	.08577	.08157	90.000	46.437	226.513
3	1	-.03648	.02651	.10944	144.000	22.393	0.000
3	2	-.05042	.06939	.08157	126.000	46.437	133.487
3	3	-.08157	.02651	.08157	162.000	46.437	226.513
4	1	-.03648	-.02651	.10944	216.000	22.393	0.000
4	2	-.08157	-.02651	.08157	198.000	46.437	133.487
4	3	-.05042	-.06939	.08157	234.000	46.437	226.513
5	1	.01393	-.04289	.10944	288.000	22.393	0.000
5	2	0.00000	-.08577	.08157	270.000	46.437	133.487
5	3	.05042	-.06939	.08157	306.000	46.437	226.513
6	1	.11806	0.00000	-.00861	0.000	94.172	180.000
6	2	.10944	.02651	.03648	13.614	72.049	296.597
6	3	.10944	-.02651	.03648	346.386	72.049	63.403
7	1	.03648	.11228	-.00861	72.000	94.172	180.000
7	2	.00861	.11228	.03648	85.614	72.049	296.597
7	3	.05903	.09590	.03648	58.386	72.049	63.403
8	1	-.09551	.06939	-.00861	144.000	94.172	180.000
8	2	-.10412	.04289	.03648	157.614	72.049	296.597
8	3	-.07296	.08577	.03648	130.386	72.049	63.403
9	1	-.09551	-.06939	-.00861	216.000	94.172	180.000
9	2	-.07296	-.08577	.03648	229.614	72.049	296.597
9	3	-.10412	-.04289	.03648	202.386	72.049	63.403
10	1	.03648	-.11228	-.00861	288.000	94.172	180.000
10	2	.05903	-.09590	.03648	301.614	72.049	296.597
10	3	.00861	-.11228	.03648	274.386	72.049	63.403
11	1	-.11806	0.00000	.00861	180.000	85.828	0.000
11	2	-.10944	.02651	-.03648	166.386	107.950	116.597
11	3	-.10944	-.02651	-.03648	193.614	107.950	243.403
12	1	-.03648	.11228	.00861	108.000	85.828	0.000
12	2	-.00861	.11228	-.03648	94.386	107.950	116.597
12	3	-.05903	.09590	-.03648	121.614	107.950	243.403
13	1	.09551	.06939	.00861	36.000	85.828	0.000
13	2	.10412	.04289	-.03648	22.386	107.950	116.597
13	3	.07296	.08577	-.03648	49.614	107.950	243.403
14	1	.09551	-.06939	.00861	324.000	85.828	0.000
14	2	.07296	-.08577	-.03648	310.386	107.950	116.597
14	3	.10412	-.04289	-.03648	337.614	107.950	243.403
15	1	-.03648	-.11228	.00861	252.000	85.828	0.000
15	2	-.05903	-.09590	-.03648	238.386	107.950	116.597
15	3	-.00861	-.11228	-.03648	265.614	107.950	243.403
16	1	-.04509	-0.00000	-.10944	180.000	157.608	180.000
16	2	-.08157	-.02651	-.08157	198.000	133.563	313.487
16	3	-.08157	.02651	-.08157	162.000	133.563	46.513
17	1	-.01393	.04289	-.10944	108.000	157.608	180.000
17	2	-.05042	.06939	-.08157	126.000	133.563	313.487
17	3	-0.00000	.08577	-.08157	90.000	133.563	46.513
18	1	.03648	.02651	-.10944	36.000	157.608	180.000
18	2	.05042	.06939	-.08157	54.000	133.563	313.487
18	3	.08157	.02651	-.08157	18.000	133.563	46.513
19	1	.03648	-.02651	-.10944	324.000	157.608	180.000
19	2	.08157	-.02651	-.08157	342.000	133.563	313.487
19	3	.05042	-.06939	-.08157	306.000	133.563	46.513
20	1	-.01393	-.04289	-.10944	252.000	157.608	180.000
20	2	-0.00000	-.08577	-.08157	270.000	133.563	313.487
20	3	-.05042	-.06939	-.08157	234.000	133.563	46.513

5. REFLECTIVITY HISTOGRAM OF SPHERE

The cube corners contributing to the reflected signal are contained in a cap whose half-angle is the cutoff angle of the cube corners. The earliest possible reflection would come from a reflector directly facing the incident beam, and the latest, from a cube corner near the cutoff angle. The apparent spread in range is the difference between the apparent reflection points for these two cases along the direction of illumination. For a reflector facing the incident beam, the apparent reflection point is a distance nL in back of the front face, where n is the index of refraction (1.457) and L is the length of the cube corner (23.3 mm). The earliest reflection point is

$$D - nL = 118.37 - 1.457 \times 23.3 = 84.47 \text{ mm}$$

from the center of the satellite. The cutoff angle θ_c of the cube corners is

$$\theta_c = \sin^{-1}\left[n \sin\left(\tan^{-1}\frac{1}{\sqrt{2}}\right)\right] = 57^\circ.27 \quad .$$

For a cube corner at the cutoff angle, the distance of the center of the front face of the reflector from the center of the satellite along the direction of illumination is given by

$$D \cos\theta_c = 118.37 \cos 57^\circ.27 = 64.00 \text{ mm}.$$

The correction for optical path length in the reflector is

$$L\sqrt{n^2 - \sin^2\theta_c} = 23.3\sqrt{1.457^2 - \sin^2 57.27} = 27.72 \text{ mm} \quad .$$

Therefore, the latest apparent reflection point is 64 - 27.72 = 36.28 mm from the satellite's center. The range difference between the earliest and the latest reflection points is 84.47 - 36.28 = 48.19 mm. Figure 3 shows the reflectivity of each 1-cm interval, in units of the equivalent number of cube corners at normal incidence, starting from the earliest reflection point. This histogram is for a direction of illumination

given by $\theta = -13°$ and $\phi = 60°$, where θ and ϕ were defined in Figure 1. For this direction, the total effective reflecting area is 3.19587 times the area of one cube corner, and the mean apparent reflection point is 73.4 mm from the center of the satellite. The cube corner shown on the histogram is in the closest possible position to the observer. (None of the cube corners points exactly at the observer for this particular direction of illumination. The earliest and latest apparent reflection points for this case are 82.2 and 41.6 mm, respectively.) Table 3 lists the percentage of the total return in each interval and the cumulative percentage, starting from the earliest reflection point.

Table 3. Percentage of return in each 1-cm interval.

Interval	Percentage of return	Cumulative percentage
1	44	44
2	38	82
3	15	97
4	2	99
5	1	100

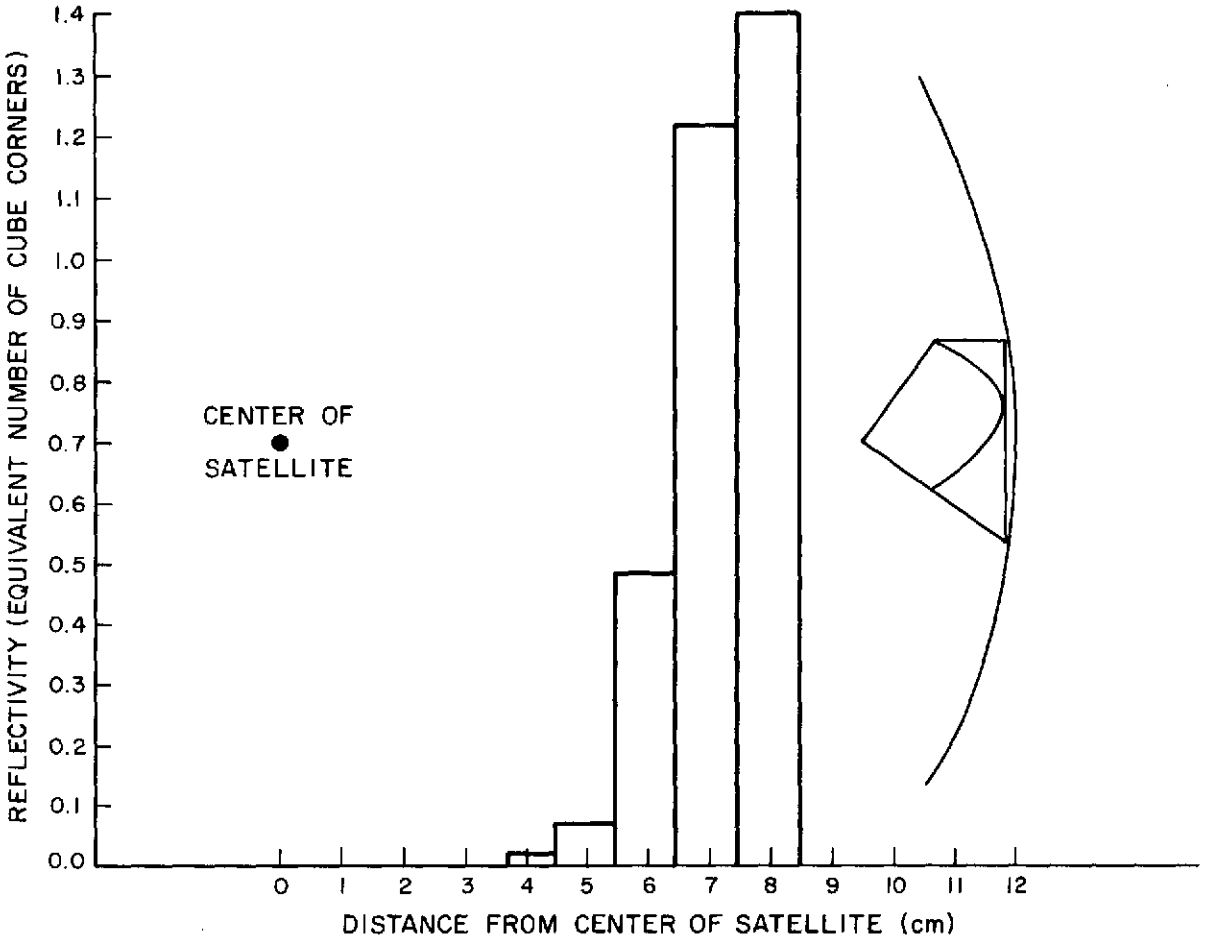

Figure 3. Reflectivity histogram of Starlette.

6. SIGNAL-STRENGTH COMPUTATION

The data contained in the tables presented later can be used to estimate signal strengths for laser ranging, by use of the following equation:

$$N = \frac{E}{h\nu} G_T A_S G_S A_R \frac{T^2}{R^4} \eta \quad ,$$

where

N = number of photoelectrons,

E = transmitted energy,

h = Planck's constant,

ν = frequency of laser light,

G_T = "gain" of transmitter,

A_S = active reflecting area of satellite,

G_S = "gain" of satellite array,

A_R = area of receiving telescope,

T = atmospheric-transmission factor,

R = range from station to satellite,

η = constant, which includes the quantum efficiency of the photomultiplier and the optical transmission factors of the transmitter, the satellite, and the receiver.

If the transmitted beam is a uniform spot of solid angle Ω_T, the "gain" function of the transmitter is

$$G_T = \frac{1}{\Omega_T} \quad .$$

The author is indebted to P. O. Minott (Goddard Space Flight Center) for pointing out that the gain functions used in this equation do not contain the factor of 4π used in the standard definition of gain. Those given in later sections can be converted to the standard definition by multiplying by 4π. Furthermore, the signal-strength equation above can be converted to the standard definition of gain by adding the factor $1/(4\pi)^2$.

7. METHOD OF COMPUTING TRANSFER FUNCTION

In computing the transfer function of the Starlette retroreflector array, the cube corners have been modeled as isothermal, geometrically perfect reflectors (except for the dihedral-angle offset) with perfect metal reflecting coatings on the back faces. The primary effect of real metal faces is a decrease in the intensity of the return signal because of the triple metallic reflection. This loss should be added to the constant η of the previous section, along with reflection losses at the front face as the beam enters and leaves the cube corners.

The computation of the range correction includes a correction for the optical path length of the ray within the cube corner. The range correction is the difference between the centroid of the actual return signal and the centroid of the return signal that would be received from a point reflector at the center of mass of the satellite. The correction listed is the one-way correction.

The gain functions and range corrections presented are for the incoherent case; that is, the intensities of the reflections are added without taking into account coherent interference among the reflected signals from the individual cube corners.

The variation of the range correction due to optical coherence has been derived by statistical analysis of a set of coherent returns constructed by assigning random phases to the reflection from each cube corner by using a pseudo random-number generator. Because the coherent variations are computed from a limited number of cases, the results should be considered as only an indication of the magnitude of the effect. The incoherent range correction is the mean value of the coherent corrections.

8. ACTIVE REFLECTING AREA AND GAIN FUNCTION

In order to calculate reflected signal strengths from the equation in Section 6, we need to find the active reflecting area A_S and the gain function G_S. The average A_S computed from a set of 25 different directions of illumination is 3.197 times the area of one cube corner at normal incidence. The root-mean-square (rms) deviation for the set is 0.056 times the area of one reflector.

Table 4 gives the gain function of the Starlette retroreflector array for two wavelengths and various dihedral-angle offsets. As stated in Section 3, the average offset of the reflected beam is 7 arcsec, which corresponds to a dihedral-angle offset of about 1.5 arcsec. The tables for 1.5 arcsec should yield the best estimate of the behavior of the array. The gain function for other offsets is given for the purpose of estimating the extremes of behavior possible within the manufacturing tolerances used for the cube corners. No attempt has been made to study variations in performance due to factors other than dihedral-angle offset.

The first column in Table 4 is the velocity aberration, in microradians, and the second gives the gain function of the array, in units of 10^7. To the right of the columns is a computer-plotted graph, in which the gain function increases to the right and the velocity aberration increases down the page. The gain function is the average value around a circle in the far field with a radius equal to the velocity aberration. The second part of each table gives the rms variation of the gain function around the circle. The computations were done for a direction of illumination given by $\theta = -13°$ and $\phi = 60°$ (see Figure 1a). We chose this direction because the active reflecting area and range correction for this particular case are close to the average values.

Table 4. "Gain" versus velocity aberration. (The gain functions presented here differ by a factor of 4π from the standard definition of gain; see Section 6.)

a) DIHEDRAL ANGLE 0.00 WAVELENGTH 6943

AVERAGE GAIN FUNCTION(1.E+7)

0	79.89
5	71.84
10	55.88
15	36.61
20	20.24
25	9.83
30	4.94
35	3.21
40	2.49
45	1.82
50	1.16

R.M.S. FLUCTUATION

0	0.00
5	.90
10	1.73
15	2.31
20	1.83
25	.73
30	.43
35	.61
40	.48
45	.47
50	.39

b) DIHEDRAL ANGLE .50 WAVELENGTH 6943

AVERAGE GAIN FUNCTION(1.E+7)

0	72.15
5	64.90
10	50.56
15	33.39
20	18.96
25	9.94
30	5.75
35	4.17
40	3.29
45	2.35
50	1.48

R.M.S. FLUCTUATION

0	0.00
5	.81
10	1.51
15	1.97
20	1.48
25	.50
30	.45
35	.53
40	.43
45	.55
50	.47

Table 4 (Cont.)

c) DIHEDRAL ANGLE 1.00 WAVELENGTH 6943

AVERAGE GAIN FUNCTION(1.E+7)

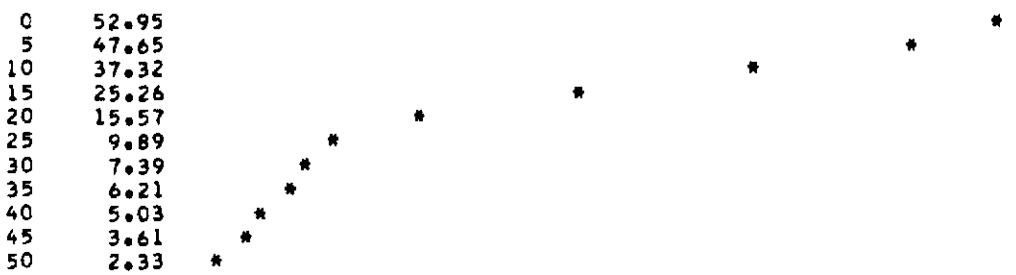

R.M.S. FLUCTUATION

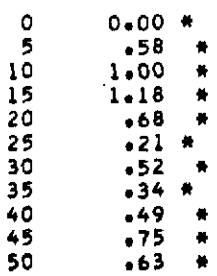

d) DIHEDRAL ANGLE 1.50 WAVELENGTH 6943

AVERAGE GAIN FUNCTION(1.E+7)

R.M.S. FLUCTUATION

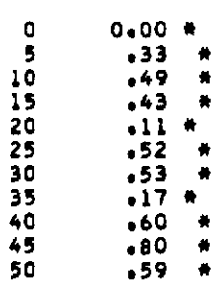

Table 4 (Cont.)

e) DIHEDRAL ANGLE 2.10 WAVELENGTH 6943

AVERAGE GAIN FUNCTION(1.E+7)

0	12.67
5	11.35
10	9.04
15	6.96
20	6.12
25	6.44
30	6.97
35	6.92
40	6.15
45	5.11
50	4.26

R.M.S. FLUCTUATION

0	0.00
5	.13
10	.16
15	.05
20	.32
25	.53
30	.36
35	.13
40	.47
45	.51
50	.41

f) DIHEDRAL ANGLE 0.00 WAVELENGTH 5300

AVERAGE GAIN FUNCTION(1.E+7)

0	137.10
5	114.35
10	74.52
15	36.46
20	14.43
25	6.60
30	4.43
35	2.91
40	1.60
45	1.00
50	.83

R.M.S. FLUCTUATION

0	0.00
5	2.43
10	3.71
15	3.19
20	.98
25	1.00
30	.82
35	.79
40	.49
45	.25
50	.22

Table 4 (Cont.)

g) DIHEDRAL ANGLE .50 WAVELENGTH 5300

AVERAGE GAIN FUNCTION(1.E+7)

0	115.06	*
5	96.06	*
10	63.18	*
15	32.46	*
20	15.27	*
25	9.15	*
30	6.71	*
35	4.31	*
40	2.31	*
45	1.34	*
50	.99	*

R.M.S. FLUCTUATION

0	0.00	*
5	2.00	*
10	2.87	*
15	2.21	*
20	.59	*
25	.88	*
30	.68	*
35	1.03	*
40	.68	*
45	.29	*
50	.22	*

h) DIHEDRAL ANGLE 1.00 WAVELENGTH 5300

AVERAGE GAIN FUNCTION(1.E+7)

0	67.31	*
5	56.32	*
10	38.16	*
15	22.77	*
20	15.56	*
25	13.12	*
30	10.58	*
35	7.11	*
40	4.29	*
45	2.79	*
50	1.99	*

R.M.S. FLUCTUATION

0	0.00	*
5	1.10	*
10	1.25	*
15	.51	*
20	.85	*
25	.59	*
30	.86	*
35	1.36	*
40	.78	*
45	.21	*
50	.23	*

Table 4 (Cont.)

i) DIHEDRAL ANGLE 1.50 WAVELENGTH 5300

AVERAGE GAIN FUNCTION(1.E+7)

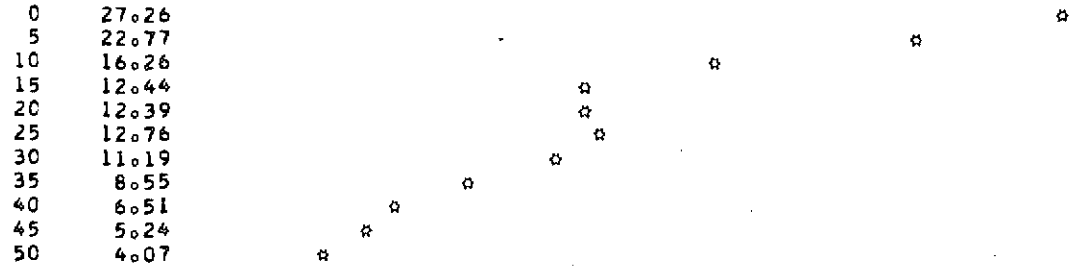

R.M.S. FLUCTUATION

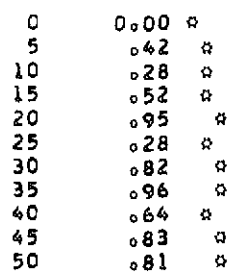

j) DIHEDRAL ANGLE 2.10 WAVELENGTH 5300

AVERAGE GAIN FUNCTION(1.E+7)

R.M.S. FLUCTUATION

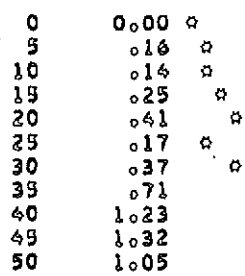

9. RANGE CORRECTION AND PULSE SPREADING

In order to utilize laser tracking data, the measured ranges must be extrapolated to the center of the satellite. The range correction that needs to be applied to the data is the difference between the centroid of the actual return signal and the centroid of the signal that would be received from a point reflector at the center of the satellite. The shape and centroid of the return signal vary from pulse to pulse owing to coherent interference, satellite orientation, and position within the far-field diffraction pattern. In order to estimate the variation of the range correction with satellite orientation, we have computed the range correction for a set of 25 satellite orientations. In these calculations, the position of each cube corner was weighted by the total reflected energy from the cube corner, which is proportional to its active reflecting area. The average range correction for the set is 0.0733 m, with an rms deviation of 0.0007 m. The range correction derived in this manner is somewhat smaller than the best estimate obtained by weighting the position of each cube corner by the intensity of its diffraction pattern.

In Table 5, the range correction, in meters, is listed in the same format and under the same conditions as the gain function of Table 4. For both wavelengths, the range correction is about 0.075 m for the average dihedral-angle offset of 1.5 arcsec.

The reflected pulse from the array will be longer, on the average, than the transmitted pulse because the cube corners are not all at the same distance from the observer. The effect is negligible except for very short pulses, such as those from mode-locked lasers. One measure of the effect is the distance of the half-power point on the leading edge from the pulse centroid. Table 6 lists the increase of this quantity for the incoherent case for three different incident-pulse lengths. The values shown are the one-way range error that would result in a half-maximum detection system. Tests made with large numbers of coherent returns do not indicate that the incoherent-pulse spreading at the half-power point is the mean of the spreading for the coherent pulses. The use of Table 6 to correct range data for pulse spreading would, therefore, be questionable.

Table 5. Range correction versus velocity aberration.

a) DIHEDRAL ANGLE 0.00 WAVELENGTH 6943

AVERAGE RANGE CORRECTION(METERS)

0	.0777
5	.0776
10	.0770
15	.0760
20	.0740
25	.0709
30	.0681
35	.0681
40	.0701
45	.0701
50	.0681

R.M.S. FLUCTUATION

0	0.0000
5	.0001
10	.0002
15	.0005
20	.0010
25	.0010
30	.0008
35	.0026
40	.0015
45	.0021
50	.0034

b) DIHEDRAL ANGLE .50 WAVELENGTH 6943

AVERAGE RANGE CORRECTION(METERS)

0	.0776
5	.0775
10	.0769
15	.0758
20	.0740
25	.0716
30	.0701
35	.0710
40	.0723
45	.0719
50	.0697

R.M.S. FLUCTUATION

0	0.0000
5	.0001
10	.0002
15	.0005
20	.0008
25	.0005
30	.0009
35	.0016
40	.0008
45	.0015
50	.0028

Table 5 (Cont.)

c) DIHEDRAL ANGLE 1.00 WAVELENGTH 6943

AVERAGE RANGE CORRECTION(METERS)

0	.0773	*
5	.0771	*
10	.0765	*
15	.0754	*
20	.0738	*
25	.0727	*
30	.0730	*
35	.0741	*
40	.0746	*
45	.0739	*
50	.0722	*

R.M.S. FLUCTUATION

0	0.0000	*
5	.0000	*
10	.0002	*
15	.0003	*
20	.0003	*
25	.0004	*
30	.0011	*
35	.0010	*
40	.0004	*
45	.0011	*
50	.0020	*

d) DIHEDRAL ANGLE 1.50 WAVELENGTH 6943

AVERAGE RANGE CORRECTION(METERS)

0	.0767	*
5	.0764	*
10	.0756	*
15	.0744	*
20	.0734	*
25	.0734	*
30	.0745	*
35	.0754	*
40	.0755	*
45	.0748	*
50	.0738	*

R.M.S. FLUCTUATION

0	0.0000	*
5	.0001	*
10	.0001	*
15	.0001	*
20	.0004	*
25	.0011	*
30	.0012	*
35	.0008	*
40	.0003	*
45	.0008	*
50	.0012	*

Table 5 (Cont.)

e) DIHEDRAL ANGLE 2.10 WAVELENGTH 6943

AVERAGE RANGE CORRECTION(METERS)

0	.0752
5	.0747
10	.0735
15	.0722
20	.0721
25	.0735
30	.0750
35	.0757
40	.0756
45	.0751
50	.0747

R.M.S. FLUCTUATION

0	0.0000
5	.0001
10	.0000
15	.0004
20	.0012
25	.0014
30	.0010
35	.0005
40	.0003
45	.0006
50	.0008

f) DIHEDRAL ANGLE 0.00 WAVELENGTH 5300

AVERAGE RANGE CORRECTION(METERS)

0	.0777
5	.0774
10	.0764
15	.0741
20	.0701
25	.0678
30	.0699
35	.0697
40	.0675
45	.0673
50	.0696

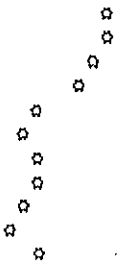

R.M.S. FLUCTUATION

0	0.0000
5	.0001
10	.0004
15	.0009
20	.0008
25	.0021
30	.0016
35	.0026
40	.0024
45	.0022
50	.0035

Table 5 (Cont.)

g) DIHEDRAL ANGLE .50 WAVELENGTH 5300

AVERAGE RANGE CORRECTION(METERS)

0	.0776
5	.0772
10	.0762
15	.0740
20	.0716
25	.0716
30	.0731
35	.0722
40	.0696
45	.0684
50	.0692

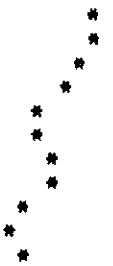

R.M.S. FLUCTUATION

0	0.0000
5	.0001
10	.0003
15	.0006
20	.0002
25	.0014
30	.0007
35	.0016
40	.0022
45	.0015
50	.0031

h) DIHEDRAL ANGLE 1.00 WAVELENGTH 5300

AVERAGE RANGE CORRECTION(METERS)

0	.0770
5	.0765
10	.0753
15	.0737
20	.0734
25	.0747
30	.0753
35	.0743
40	.0728
45	.0720
50	.0717

R.M.S. FLUCTUATION

0	0.0000
5	.0001
10	.0002
15	.0001
20	.0010
25	.0010
30	.0004
35	.0011
40	.0014
45	.0017
50	.0023

Table 5 (Cont.)

i) DIHEDRAL ANGLE 1.50 WAVELENGTH 5300

AVERAGE RANGE CORRECTION(METERS)

0	.0756
5	.0748
10	.0732
15	.0725
20	.0740
25	.0754
30	.0757
35	.0750
40	.0745
45	.0744
50	.0742

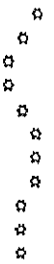

R.M.S. FLUCTUATION

0	0.0000
5	.0001
10	.0001
15	.0010
20	.0013
25	.0008
30	.0003
35	.0007
40	.0010
45	.0014
50	.0016

j) DIHEDRAL ANGLE 2.10 WAVELENGTH 5300

AVERAGE RANGE CORRECTION(METERS)

0	.0742
5	.0725
10	.0693
15	.0698
20	.0728
25	.0744
30	.0745
35	.0745
40	.0750
45	.0755
50	.0755

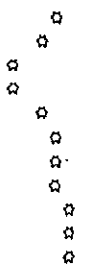

R.M.S. FLUCTUATION

0	0.0000
5	.0002
10	.0002
15	.0012
20	.0010
25	.0002
30	.0003
35	.0006
40	.0009
45	.0008
50	.0005

Table 6. Pulse spreading.

Pulse width (nsec)	Pulse spreading (m)
20.0	0.0000
5.0	0.0002
0.2	0.0040

10. INFLUENCE OF OPTICAL COHERENCE

Because of coherent interference between the reflections, the strength, centroid, and shape of the laser echo from the Starlette satellite vary from pulse to pulse. To estimate the fluctuation in measured range due to interference, we have computed sets of coherent pulses for three different transmitted pulse lengths (see Table 7). The pulse length is given in the first column (half-power, full width), and the rms variation of the measured range for two types of weighting appears in columns 2 and 3. In the second column, all pulses are weighted equally; this procedure gives larger variations owing to the fact that weaker pulses tend to have greater variations in centroid. In the third column, each pulse is weighted by the ratio of the strength of the coherent pulse to the average (or incoherent) signal strength. The numbers should be considered only approximate since each rms variation was derived from statistical analysis of a set of 100 coherent returns. In general, the variations decrease as the pulse length decreases.

Table 7. Coherent range variations.

Pulse length (nsec)	Equal weighting (m)	Weighted by signal strength (m)
20.0	0.0127	0.0072
5.0	0.0140	0.0044
0.2	0.0068	0.0052

When plotted versus time, the reflected pulses from the Starlette array will have nearly the same shape as the transmitted pulse except for the 0.2-nsec transmitted pulse length. As shown in Table 6, the reflected pulse will be significantly longer in this case as a result of the difference in range to individual cube corners. In addition, the shape of the pulse may occasionally show two peaks as a function of time, owing to coherent interference.

11. ACCURACY OF RANGE CORRECTION

As can be seen from the reflectivity histogram of Figure 3, the spread in range of the reflectors contributing to the return signal is only a few centimeters. In fact, over 80% of the reflected energy comes from an area only 2 cm wide, and 97% is received from a region only 3 cm wide (see Table 3). The range uncertainty due to satellite geometry cannot be greater than about 1 or 1.5 cm.

In Table 8, the range correction is given as a function of dihedral-angle offset of the cube corners. The numbers were obtained by averaging the values from Table 5 over the 30- to 50-μrad range of velocity aberration.

Table 8. Range correction versus dihedral-angle offset.

Dihedral-angle offset (arcsec)	Wavelength 6943	Wavelength 5300
0	0.0689	0.0688
0.5	0.0710	0.0705
1.0	0.0736	0.0732
1.5	0.0748	0.0748
2.1	0.0752	0.0750

The range correction decreases as the dihedral angle decreases. None of the values is significantly larger than the 0.075 m we took as the best estimate of the range correction. A dihedral-angle offset of 0 arcsec shows the largest difference (about 6 mm) from the 0.075-m value. Since the range corrections for the larger dihedral-angle offsets differ by only a few millimeters, and because it is extremely unlikely that all the offsets are very small, the uncertainty in the computed range correction due to differences in beam divergence among the cube corners is probably less than 0.5 cm.

12. ACKNOWLEDGMENTS

The author wishes to express his appreciation to M. LeFebvre and G. Brachet of the Centre National d'Etudes Spatiales for providing technical data on the Starlette retroreflector array.